The edible mushroom *Albatrellus ovinus* contains a α-L-fuco-α-D-galactan, α-D-glucan, a branched (1→6)-β-D-glucan and a branched (1→3)-β-D-glucan

Anne Berit C. Samuelsen[a*], Frode Rise[b], Alistair L. Wilkins[c], Lioubov Teveleva[a], Anna Armika Tussilago Nyman[a,] and Finn L. Aachmann[d]

[a]School of Pharmacy, University of Oslo, P.O.Box 1068 Blindern, NO-0316 Oslo, Norway
[b]Department of Chemistry, University of Oslo, P.O.Box 1033 Blindern, NO-0315 Oslo, Norway
[c]School of Science and Engineering, University of Waikati, Private Bag 3105, Hamilton 3240, New Zealand
[d]Department of Biotechnology and Food Science, NOBIPOL, NTNU Norwegian University of Science and Technology, NO-7491 Trondheim, Norway

*Corresponding author E-mail address: a.b.c.samuelsen@farmasi.uio.no

Abstract

Albatrellus ovinus, the sheep polypore, is a large, dense mushroom being rich in cell wall material. Polysaccharides were isolated by sequential extraction, enzymatic treatment and analyzed with respect to monosaccharide composition, glycosidic linkages by methylation and GC-MS as well as NMR spectroscopy. A fucogalactan composed of an (1→6)-α-D-galactan backbone with single α-L-Fuc*p* residues attached at *O*-2 was identified in the hot water extract obtained after treatment with a protease and size exclusion chromatography. Both the hot water extract and the hot alkali extract contained an (1→4)-α-D-glucan whereas β-D-glucans were mainly present in the latter. Structural analysis suggested the presence of two different β-D-glucan backbone structures; a (1→6)-linked β-D-glucan with single β-D-Glc*p* residues at *O*-3 and also a (1→3)-linked β-D-glucan with branches in O-6. In addition there were identified short (1→2)-linked β-D-xylan and (1→3)-α-D-mannan chains.

Keywords: *Albatrellus ovinus*, fucogalactan, β-glucan, α-glucan

1. Introduction

Wild edible mushrooms have been part of the human diet for centuries due to their availability in nature as well as their culinary and nutritional aspects. Common edible mushrooms are rich in proteins (16-37% of dry weight (dw)), dietary fibre (24-47 % dw), and contain low amounts of fat (1-2 % dw) [1]. Mushrooms are also sources of minerals and vitamins [1, 2], phenolic compounds and terpenoids [2, 3]. *Albatrellus ovinus* (sheep polypore) is a polypore and a mycorrhizal fungus that lives in symbiosis with conifers, most often the Norwegian spruce. It is an edible mushroom with a white to tan fruiting body cap that can grow quite large, up to 25 cm in diameter. The flesh appears brittle, quite dense, and becomes yellow upon frying or scratching. This mushroom does not have any distinct odor or taste and is not

considered amongst the most valuable mushrooms. However, due to its mild taste, it is quite useful to mix with other mushrooms. The size of the fruiting body also indicates that this mushroom could be a rich source of cell wall components.

In general, the fungal cell wall is composed of inner layers of chitin and β-D-glucans [4, 5]. The β-D-glucans are typically (1→3)- and/or (1→6)-linked chains with varying amounts of side chains in position *O*-6 or *O*-3 as listed in several review articles [6-9]. β-D-glucans have attracted special interest as they are potentially recognized by the human immune system and considered immune modulating substances [10-13]. Several other activities have been reported including hypoglycaemic effect[14], effect against obesity[15], antiviral activity[7], antitumor [8] and even antioxidant activity [16]. The outer layers of the fungal cell wall contain branched polymers in which structures are species dependent; branched D-mannans are found in microfungi such as *Candida albicans* [4] and *Saccharomyces cerevisae* [17] as well as in the fruiting bodies of for instance *Cantharellus cibarius* [18]. Other species contain D-galactans or hetero-D-glycans typically composed of D-xylose, D-mannose, D-galactose and L-fucose monomers [8]. Specific examples include the fucogalactan found in *Agaricus bisporus* [19], the fucomannogalactan from *Amanita muscaria* [20] and a heterogalactan found in *Flammulina velutipes* reported to contain both D-mannose, D-glucose and L-fucose in the side chains [21]. In addition, β-D-glucans with (1→3)-, (1→4)- or (1→6)-linkages have been identified in several fungi [6].

A. ovinus is considered non-poisonous and contains massive amounts of unexplored cell wall material, which is why we wanted to map the different types of polysaccharide structure motives present in its fruiting bodies. This in-depth separation and characterization of the polysaccharides will also potentially reveal if it contains rare or new structures not reported previously. Previous studies on *A. ovinus* (syn. *Polyporus ovinus* Schaeff.) polysaccharides are limited, we only identified one single study from 1969 that reported on a fucogalactan from the water extract [22]. Here we present the sequential extraction of dried *A.ovinus* fruiting bodies using solvents of increasing polarity followed by structure elucidation revealing that there are at least four different types of non-chitin-polysaccharides in this mushroom.

2. Results and Discussion

Dried and milled fruiting bodies of *Albatrellus ovinus* were extracted according to the flow diagram in Fig. 1. The hot water extract (WAo) yielded 1.9% while the alkali extract (AAo) constituted 12.5 % of the dry starting material. The AAo extract was further fractionated into a water insoluble fraction AAoI (58 %) and a water soluble fraction AAoS (42 %) that was recovered by ethanol precipitation. AAoS was further fractionated by re-solubilization in water.

2.1 The fucogalactan in WAoF1

The hot water extract WAo consisted of two main size populations (Fig 2a, upper trace) that could be separated and prepared by SEC on a preparative Sephacryl S-500 column to fraction WAoF1 and WAoF2.

Analytical SEC on a TSK-Gel column revealed that the molecular weight of WAoF1 at the highest peak (Mp) was 251 kDa relative to pullulan standards. The second fraction, WAoF2 (Fig. 2a, lower trace) contained the lower molecular weight fraction (Mp 12.4 kDa) of the water extract.

Analysis of WAo on SEC-MALLS (Fig 2b) of WA0 showed higher weight average molecular mass (Mw) of both fractions; 665 kDa and 34 kDa, respectively, both with a narrow molecular mass distribution (Mw/Mn= 1.001 and 1.07). The low intensity RI signals in front of the main peak of WAoF1 were from aggregates due to the combination of the very large light scattering signal and a small RI signal in SEC-MALLS.

Fraction WAoF1 and WAoF2 contained D-Gal, L-Fuc, D-Glc and D-Man, in the ratio (60:15:20:5) and (22:6:69:3), respectively. Linkage analysis by methylation and GC-MS revealed that all monomers were in the pyranose form (*p*). The D-Gal*p* residues were (1→6)-linked with branching in position *O*-2 in about one third of the monomers (Table 1). However, only very small amounts of non-reducing D-Gal*p*-(1→ residues were detected which strongly indicated the presence of a heterogalactan. The amounts of L-Fuc*p*-(1→ residues corresponded well to the amounts of D-Gal*p*-branching residues. Based on these results it was proposed that the water extract, and in particular SEC-fraction WAoF1, contained a fucogalactan which was also in accordance to the mentioned previous study [22].

Small amounts of D-Glc*p* residues in WAoF1 were identified having several different types of linkages; →3)-D-Glc*p*-(1→, →3,6)-D-Glc*p*-(1→, and →6)-D-Glc*p*-(1→, →4)-D-Glc*p*-(1→, and →4,6)-D-Glc*p*-(1→, and were attributed to co-extracted (1→3)-/(1→6)- and (1→4)-/(1→6)-D-glucans. SEC-HPLC of WAoF1 (Fig 2.) indicated that the isolated material contained small amounts of WAoF2. WAoF2 contained 70% D-Glc residues with the same type of linkages as those found in trace amounts in WAoF1.

NMR experiments supported the presence of a fucogalactan in WAoF1. Its structure was identified through 1D ^{1}H- and ^{13}C-NMR as well as 2D COSY, TOCSY, NOESY, HSQC and HMBC experiments. The ^{1}H NMR spectrum (Fig 3a) showed three signals at 5.08, 5.05 and 4.99 ppm in the α-anomeric region [23]. The signal at 5.08 ppm was from α-L-Fuc*p* while signals at 5.05 and 4.99 ppm appeared from two differently linked α-D-Gal*p* residues. Two main anomeric signals at 104.3 and 101.0 ppm were detected in the ^{13}C-NMR spectrum (Fig 3b). In addition, a signal at 18.6 ppm was also observed being typical for the methyl group of a 6-deoxy sugar. The methyl signal was also observed in the ^{1}H NMR spectrum, as a doublet at 1.25 ppm. Based on GC retention times of TMS derivatives after methanolysis this deoxy sugar was identified as L-Fuc*p*.

Further assignments of the individual sugar residues were performed by analyzing COSY and TOCSY spectra (not shown) with aid of literature values for similar structures [19, 24, 25]. TOCSY correlations identified confirmed the H-1, H-2, H-3 and H-4 signals of an α-L-Fuc*p* spin system (not shown). The Nuclear Overhauser Effect (NOE) correlation peaks observed (Table 2) were consistent with those required for an α-L-Fuc*p* residue. ^{13}C NMR signals at 71.3, 72.6, 74.7 and 70.1 ppm were identified as C-2, C-3, C-4 and C-5 on α-L-Fuc*p*-(1→, respectively via correlations observed in a HSQC spectrum (Fig. 4a). There were no indications of glycosidic linkages to other sugar moieties other than through the anomeric carbon of the α-L-Fuc*p* residues which was in agreement with linkage analysis by methylation (Table 1).

The α-Gal*p* residues were the main constituents in WAoF1. The ^{1}H-signals from H-2 in monomer type b at 3.86 ppm (b2 in Fig.4a) and monomer type c (c2) at 3.84 ppm were identified through COSY correlations with their respective anomeric protons. Other signal assignments (Fig 4a and Table 2) were elucidated via COSY and TOCSY correlations and are consistent with those found in literature for similar structures [19, 24, 25]. TOCSY correlations confirmed the identification of H-2, H-3 and H-4. The absence of an observable correlation between H-4 and H-5 can be attributed to the small coupling between H-4 and H-5 in D-Gal*p* [23]. Intra-residual NOE correlations between protons on b1 and b2 as well as b3-b5 and b3-b4 were consistent with the α-anomeric configuration of the galactose residues [23]. ^{13}C NMR signals at 71.2, 72.6, 72.5 and 71.8 ppm were identified as carbons b2, b3, b4 and b5, respectively. The b6 signal was identified in the multiplicity-edited HSQC spectrum at 69.6 ppm (Fig. 4a). The chemical shift of this signal showed that *O*-6 was involved in a glycosidic linkage [26]. Furthermore, NOE correlations between the anomeric proton on b1 (4.99 ppm) and the pair of b6 protons (3.92 and 3.70 ppm) across the glycosidic linkage as well as an inter-residual HMBC three bond correlation between protons on b1 and carbon b6 (Fig.4b) demonstrated the presence of →6)-α-D-Gal*p*-(1→ residues in a polymer. Thus, monomer b was identified as →6)-α-D-Gal*p*-(1→ occurring in a (1→6)-linked α-D-galactan.
^{13}C-signals appearing at 80.8, 71.4, 72.6, 72.2 and 70.3 ppm were assigned to carbons on residue c; c2, c3, c4, c5 and c6, respectively. The glycosylation shifting of the C-2 and C-6 signals downfield indicated substitution in these positions. Thus, monomer c was identified as →2,6)-α-D-Gal*p*-(1→. Interestingly, there was observed NOE and HMBC inter-residue correlations between c1 and c6 showing that →2,6)-α-D-Gal*p*-(1→ residues occurred adjacent to one another in the polymer. In addition, it was found that residues b and c occurred next to one another in the polymer as well, due to NOE correlations between b1 and c6 and HMBC correlations between c1 and b6. Additional partly resolved H/C-6 cross peaks were observed at 3.89/69.8 and 3.74/69.8 ppm (Fig.4b) which probably are correlation between residue c being substituted by b. Taken together, the (1→6)-linked α-D-galactan seemed to have a random pattern of substitution in position *O*-2. The HMBC correlation peak at 5.08/80.8 ppm (Fig.4b) showed that c was substituted by α-L-Fuc*p*-(1→ in *O*-2. This was further supported by NOE correlations between the protons at c2 and a1 (a= α-L-Fuc*p*) (Table 2).

The three types of monomers α-L-Fuc*p*-(1→, →6)-α-D-Gal*p*-(1→ and →2,6)-α-D-Gal*p*-(1→occurred in the ratio 1:2:1 in the ^{1}H NMR spectrum. Based on the above data, a representative structure of the fucogalactan is proposed (Fig 4c). According to the extraction yields, the dry fruiting body of *A. ovinus* contains about 1 % (w/w) fucogalactan.

A previous study described a fucogalactan isolated from *A.ovinus* having Fuc:Gal ratio 1:3.5 [22] which is close to the ratio found in fraction WAoF1 in the present study (1:3 in ^{1}H-NMR, 1:4 by methanolysis). However, the distribution of L-Fuc*p* branches was interpreted somewhat differently in our present study where NMR correlations revealed that *O*-2 substituted (1→6)-linked α-D-Gal*p* monomers occurred both as neighbors and separated by non-substituted D-Gal*p* residues.

A.ovinus is not the only *Basidiomycota* containing a fucogalactan. Fucogalactans have been isolated from the edible *Coprinus comatus* (Fuc:Gal ratio 1:4) [25] and the Chinese medicinal mushroom *Hericium erinaceus* (Fuc:Gal 1:4) [24]. Fucogalactans that contain an *O*-methylated residue have been described in *Lactarius rufus* [27] and *Agaricus bisporus* [19, 27, 28], and even more complex heterogalactans such as

the fucomannogalactan from *Grifola frondosa* [29] have been reported. Heterogalactans and other mushroom derived heteropolysaccharides appear quite common, and previously reported structures are listed in a recent review [30].

2.2 D-glucans

AAoS and AAoI both contained 80 % Glc*p* while WAo contained 40 % Glc*p* according to GC analysis of its methylglycosides after methanolysis. Linkage analysis showed presence of 4)-D-Glc*p*-(1→, 4,6) -D-Glc*p*-(1→, →3)-D-Glc*p*-(1→, →6)-D-Glc*p*-(1→, and →3,6)-D-Glc*p*-(1→ residues (Table 1a and b).

2.2.1 α-D-glucan

The water extract WAo as well as both alkali extracts AAoS and AAoI, contained significant amounts of →4)-D-Glc*p*-(1→ residues. The extracts reacted with the iodine-KI reagent which is the classical chemical test for presence of starch or glycogen. In essence, the reagent forms polyiodides (I_n^{m-}) which enter the (1→4)-α-D-glucan helix forming a blue-black colored complex [31]. The reaction therefore indicated that the detected →4)-D-Glc*p*-(1→ residues were of the α-anomeric configuration. Furthermore, the →4)-D-Glc*p*-(1→ residues were susceptible to hydrolysis with amylase (EC 3.2.1.1) which hydrolyses (1→4)-linkages of α-D-glucans. Treatment with amylase hydrolysed 50-60 % of the →4)-D-Glc*p*-(1→ residues present. Incomplete enzymatic hydrolysis with the amylase was attributed to the presence of hydrolysis resistant side chains in position *O*-6 as well as possible interactions and entanglements with other polysaccharides. However, the enzymatic activity confirmed the presence of a starch- or glycogen-like polysaccharide.

It was found that a fraction of the water extract (WAo) could bind to immobilized Concanavalin A (ConA) by affinity chromatography. ConA is a lectin that binds molecules containing D-Glc*p* residues of the α-anomeric configuration [32] rather than β-D-Glc*p* residues. Analysis of the ConA binding fraction of WAo (designated WAoConA+, Table 1a) revealed high amounts of →4)-D-Glc*p*-(1→ and →4,6)-D-Glc*p*-(1→ residues. This method was not applicable to the alkali extracts due to limited water solubility. NMR analysis of the ConA binding fraction could confirm the presence of a (1→4)/(1→4,6)-linked glycogen-like polysaccharide (Table 3). There were two main anomeric signals in the α-anomeric region of HSQC spectrum; at 5.36/103.2 ppm and at 5.36/103.2 ppm appearing from H/C-1 of →4)-α-D-Glc*p*-(1→ and →4,6)-α-D-Glc*p*-(1→,respectively (Spectra not shown). ^{13}C signals from C-2, C-3, C-4, C-5 and C-6 in →4)-α-D-Glc*p*-(1→ residues appeared at 74.9, 76.6, 81.2, 74.5 and 64.0 ppm, respectively. NOE inter-residual correlations between H-1 and H-4 and HMBC three bond correlations between H-1 and C-4 confirmed the (1→4)-linkages. Weak C-6 signals appeared at 70.7 ppm due to side chains at *O*-6 of the (1→4)-linked backbone. An additional HSQC cross peak at 3.43/72.8 ppm was from H/C-4 in α-D-Glc*p* non-reducing ends. All signals were identical to those detected in reference spectra obtained from purchased amylose (Table 3) as well as previously reported chemical shift values from HSQC analysis of amylose [33] and chemical shift predictions of amylose provided by the Widmalm Research Group [34]. The degree of branching was estimated from the →4)-α-D-Glc*p*-(1→ / →4,6)-α-D-Glc*p*-(1→ ratio. This ratio was found to be 3.4 by integration of ^{1}H-NMR anomeric signals and 4.3 by methylation analysis, indicating that side chains were appearing in average on every 4th →4)-α-D-Glc*p*-(1→ unit (Fig. 6a).

According to linkage analysis lyophilized *A. ovinus* fruiting bodies contain 1.9 % (w/w) α-D-glucan. The α-D-glucan appeared in all fractions, suggesting it to be present in the mushroom from the innermost water insoluble β-D-glucan layer to the water soluble branched fucogalactan in the cell wall outer region.

(1→4)-α-D-glucans have been identified in other edible mushrooms such as the oyster mushroom (*Pleurotus ostreatus*) [35], and the common champignon (*Agaricus bisporus*) [36] while maitake (*Grifola frondosa*) is reported to contain a branched glycogen-like D-glucan [37].

The fraction of WAo which did not bind ConA (designated WAoConA- in Table 1.) contained fucogalactan as well as →3)-D-Glc*p*-(1→ residues which turned out to be of the β-anomeric configuration.

2.2.2 β-D-glucans

The water insoluble and water soluble alkali extracts (AAoI and AAoS) both contained about 80 % Glc in addition to 10 % Man, 4 % Xyl, 2 % Fuc and 2 % Gal. For further fractionation, a procedure of re-dissolving and re-precipitation was conducted (Fig.1). Briefly, AAoS was dissolved in hot water, sonicated, precipitated with ethanol, followed by repeatedly washing of the precipitate with 70% ethanol. The obtained fraction was designated AAoSP and appeared to contain 93 % Glc. Linkage analysis revealed presence of D-Glc*p*-(1→, →3)-D-Glc*p*-(1→, →6)-D-Glc*p*-(1→, and →3,6)-D-Glc*p*-(1→ residues (Table 1b).

2D NMR (HSQC, HMBC, TOCSY and COSY) spectra of AAoSP were interpreted with the support from reference spectra of a yeast derived β-D-glucan [18] and literature data [18, 34, 38, 39]. The HSQC spectrum of AAoSP in Fig. 5a is shown with somewhat reduced signal intensity to highlight the dominating β-D-Glc*p* signals and make other minor sugars less prominent. The anomeric ^{1}H and ^{13}C NMR signals at 4.72/106.1, 4.79/105.8, 4.53/106.2 and 4.56/106.0 ppm corresponded to β-D-Glc*p*-(1→, →3)-β-D-Glc*p*-(1→, →6)-β-D-Glc*p*-(1→, and →3,6)-β-D-Glc*p*-(1→, respectively (labelled d1, e1, f1 and g1 in Fig. 5a) [18]. Complete assignments of the individual sugar residues are presented in Table 4 and Fig 5a.

HSQC spectra data indicated the presence of significant amounts of →6)-β-D-Glc*p*-(1→ residues (labeled fin Fig. 5a). Substitution in position *O*-6 leads to more deshielded chemical shift of C-6 signals at 72.2 ppm (f6 Fig.5a), and HMBC correlations between H-1 and C-6 across the glycosidic linkage (Table 4) confirmed the presence of (1→6)-linked chains. The (1→6)-linked β-D-glucan chains appeared to be branched with single D-Glc*p* residues: H-1 of the D-Glc*p* non-reducing ends (d1) showed three bond HMBC correlations with C-3 on →3,6)-β-D-Glc*p*-(1→ (g3). In addition, there were d1-g3 inter-residue NOE correlations. Thus, single D-Glc*p* residues appeared linked to *O*-3 on the (1→6)-β-D-glucan chain. Additional inter-residue NOE correlations between g1-g6 indicated presence of branched β-D-Glc*p* residues adjacent to one another in the main chain.

According to methylation analysis, →3)-D-Glc*p*-(1→ was the dominating sugar monomer in AAoSP. In NMR, the characteristic ^{13}C-signals from *O*-3 substituted D-Glc*p* results in a more deshielded chemical shift at 87.8 ppm. The corresponding H/C-3 cross peak in HSQC is labeled e3 in Fig 5a. HMBC three

bond correlations between the proton on e1 and carbon on e3, and also e1-e3 NOE correlations (Table 4) confirmed presence of a (1→3)-linked β-D-glucan. H-1 of D-Glc*p* non-reducing ends (d1 Fig.5a) showed HMBC correlation to C-3 on →3)-β-D-Glc*p*(1→ (e3) as well as NOE correlations between d1 and e3 indicating a moderate degree of polymerization.

The ^{13}C signal at 88.3 ppm was assigned to C-3 of →3,6)-D-Glc*p*-(1→ (g3 Fig.5a). HMBC correlations between proton on g1 and carbon on e3 indicated that the (1→3)-linked main chain had certain degree of branching in *O*-6. However, the nature of those side chains could not be identified at since neither HMBC nor NOE correlations were observed between the →3,6)-β-D-Glc*p*-(1→ branching points and other sugar residues were detectable.

Small amounts of D-Xyl and D-Man appeared in several fractions and in particular in the alkali fractions. The highest amounts were detected in AAoSSp which, according to methanolysis and GC, contained 25 % D-Man and 7 % D-Xyl in addition to D-Glc. Methylation analysis revealed that all monomers were in the pyranose form, and the D-Man*p* residues were →3)-D-Man*p*-(1→ linked whereas the D-Xyl*p* residues were D-Xyl*p*-(1→ and →2)-D-Xyl*p*-(1→ -linked (Table 1b).
In the HSQC spectrum the anomeric H/C correlation peak at 5.16/104.9 ppm was assigned to D-Man*p* (h1 Fig.5b) [34]. The anomeric ^{13}C-^{1}H-coupling constant $^{1}J_{(C1,H1)}$ was 169 Hz, i.e. close to 170 Hz which is characteristic for the equatorial position of H1. Thus, the D-Man*p* residues were in the α-anomeric configuration [23]. The H/C-2 cross peak at 4.25/73.0 ppm was identified by COSY and TOCSY whereas the peak from substituted *O*-3 on D-Man*p* at 4.03/81.4 ppm was deduced from COSY correlations as well as by comparisons with theoretical predicted values [34] and data from literature [40]. Strong inter-residual NOE correlations, selective NOESY and ROESY between h1 and h3 (not shown) and the observed h1/h3 HMBC cross peak (Fig 5b) confirmed this linkage. The identification of H/C-5 in →3)-α-D-Man*p*-(1→ was confirmed by a strong HMBC correlation signal between h1and h5. Selective 1D NOESY experiments were performed in order to reveal the nature of the weak additional upper HMBC cross peak at 5.16/72.8 ppm (Fig. 5b). The corresponding HSQC signals were overlapping and could either be from h2 or f/g6. In selective 1D NOESY, only the ^{1}H-signals that correlate with the signal selected (e.g. H on h1) are seen, and in this case we found that the proton on h1 correlated with h2, not f/g6. Thus, the upper HMBC cross peak from h1was a four bond correlation to C-2 on h2.

D-Man*p*-(1→ non-reducing ends tend not to be separated from non-reducing ends of D-Glc*p* in methylation analysis. However, H/C cross peaks in HSQC indicated presence of α-D-Man*p*-(1→ residues (h' in Fig. 5b) were h'1 appeared at 5.18/104.5 ppm and h3 from α-D-Man*p* residues linked to the non-reducing ends at 4.05/72.8 ppm [40]. HMBC correlation between H-1 on h'1 and C-3 of →3)-α-D-Man*p*-(1→ showed that the non-reducing D-Man*p* residues were attached to *O*-3 in mannan chain, thereby indicating that the (1→3)-linked α-D-mannan chains were relatively short.

In addition there were anomeric H/C-signals at 4.43/106.7 ppm appearing from D-Xyl*p*-(1→ residues (residue i) (i1 Fig.5b), with $^{1}J_{(C1,H1)}$ = 160.6 Hz which is close to 160 Hz and characteristic for the β-anomeric configuration [23]. The i2 HSQC cross peak was identified by COSY correlations (3.3/76.8 ppm), and i3 appeared at 3.47/78.9 ppm. NOE correlations between i1and i3 and i5 are typical for the β-D-Xyl*p* conformation. The protons on i1 also showed both 2D NOE-correlations as well as in selective 1D NOE with j2 (Table 4). Cross peak j2 appeared from H-2 of →2)-β-D-Xyl*p*-(1→ residues (j). These residues were detected, both by methylation analysis as well as by NMR. Anomeric signals from j

appeared at 4.47/104.6 ppm (j1 Fig.5b) [34], and j2 signals (3.48/81.6 ppm, Fig.5b) were identified by COSY. Observed HMBC inter-residue correlations between j1 and j2 could indicate that the →2)-β-D-Xyl*p*-(1→ residues occurred in chains, and correlation with i1 showed that the β-D-xylan chain had a β-D-Xyl*p* residue in the non-reducing end. However, sufficient evidence of the (1→2)-linked β-D-xylan chains being part of the mannan and/or the β-D-glucans present could not be found.

AAoSSp contained significant amounts (27 %) of β-glucan (Table 1b), and NMR analysis revealed presence of β-D-Glc*p*-(1→, →3)-β-D-Glc*p*-(1→, →6)-β-D-Glc*p*-(1→ and →3,6)-β-D-Glc*p*-(1→ residues (d-g Fig.5b), i.e. the same type of β-glucan linkages as those identified in AAoSP (Fig. 5a). Two separate H/C-3 cross peaks from *O*-3 substituted β-D-Glc*p* residues were identified by in a band selective HSQC spectrum (inlay Fig. 5b). A low intensity cross peak (g3) from H/C-3 on →3,6)-β-D-Glc*p*-(1→ correlated with H1 on non-reducing D-Glc*p* ends in HMBC. Thus, the non-reducing D-Glc*p* residues appeared to be linked to *O*-3 on a (1→6)-linked β-D-glucan chain. This was the same polysaccharide structure that was found in AAoSP, and its proposed structure is presented in Fig.6b.

The upper cross peak (e3 in Fig. 5b) from H/C-3 of →3)-β-D-Glc*p*-(1→ showed intra- and inter-residual HMBC correlations with H-1 on →3)-β-D-Glc*p*-(1→ due to presence of (1→3)-β-D-glucan chains. These chains appeared to be relatively short since additional HMBC correlations between e3 and d1 were observed. As in the above discussion of β-D-glucans in AAoSP, there were no indications of single β-D-Glc*p* or polymeric β-D-glucan branches linked to the (1→3)-β-D-glucan main chain found. We believe that the (1→3)-linked glucan was of the same type in AAoSP and in AAoSSp, but the nature of the side chains remain unknown due to lack of significant correlation signals in NMR. Theoretically side chains may be β-D-xylans and/or α-D-mannans, but this remains to be determined in detail in future.

Mushroom hetero (1→3)-β-D-glucan structures have been proposed previously; e.g. a xyloglucan from *Cantharellus cibarius* [18] and a galactoglucan from *Pleurotus ostreatus* [41]. There are almost infinite possibilities of sidechain compositions in a hetero (1→3)-β-D-glucan even with the limited number of contributing monomers that are commonly found in mushrooms (D-Man, D-Gal, D-Glc, D-Xyl, L-Fuc). Sidechains may occur at different positions (*O*-2, *O*-4 or *O*-6), having different types of glycosidic linkages, monosaccharide compositions as well as in length and distribution. Mushroom derived (1→3)-β-D-glucans are often described as (1→3)-linked β-D-glucans with single sidechains in position *O*-6, such as lentinan [16], schizophyllan [42] and pleuran [43]. However, this structure appears not to be universal amongst the Basidiomycota, as there are mushrooms such as *A. ovinus* that does not contain this type of β-D-glucan. In fact, it turns out from the present study and others that the structural diversity of cell wall polysaccharides in macro fungi is enormous. Furthermore, future activity studies on new polysaccharide structures may reveal effects other than those previously reported from lentinan and schizophyllan [16, 42].

In general, the fungal cell wall is composed of β-D-glucans and chitin as well as glycoproteins forming a network [44] which makes it extremely rigid and resistant to enzymatic attack and large differences in osmotic pressure [45]. Isolation of cell wall polysaccharides is therefore seldom straightforward and requires glycosidic linkages to be broken and strong inter-molecular forces to be disrupted. Additional challenges occur due to low water solubility of polymers such as the β-D-glucans and in particular the (1→3)-β-D-glucans with low degree of branching. To overcome these issues, cell wall material is treated

with hot alkali solutions after extraction with water for isolation of water soluble polymers such as (1→6)-α-D-mannans [18] or (1→6)-α-D-galactans. Due to strong interactions and associations or even covalent linkages between polysaccharides, it is almost impossible to isolate a single type of polysaccharide totally free of co-extracted material from other types of polymers [18]. However, even not completely separated, it was still possible to determine the structural composition of four different types of polysaccharides present in the *A. ovinus* cell wall including a well characterized fuco-(1→6)-α-D-galactan, a (1→4)-α-D-glucan, a (1→6)-β-D-glucan and a (1→3)-linked β-D-glucan with yet undefined side chains appearing in *O*-6.

3. Material and Methods

The fruiting bodies of *Albatrellus ovinus* were collected in the Oslo forest and identified by Prof. Klaus Høiland at University of Oslo. A voucher sample was lyophilized and deposited for future reference.

3.1 Extraction

Fruiting bodies were rinsed mechanically, cut into smaller pieces, lyophilized and milled in a blender. Then 100 g of dry material was extracted twice with dichloromethane (1000 mL) under gentle stirring at 25°C for 24h in order to remove non-polar components (Fig.1). The residue was then subjected to Soxhlet extraction with ethanol until colorless extraction solvent, and the remaining residue was dried in air before treatment twice with boiling water (2000 mL) under reflux for 6h each time. The water extract was treated with 100 mg pancreatin from porcine pancreas (Sigma-Aldrich) for 3h at 40°C, and then the enzyme activity was terminated by boiling for 10 min, three volumes of ethanol was added and the mixture was left for precipitation at 4°C over night. The precipitate was isolated by centrifugation at 3000 rpm for 15 min on a Multifuge® 4KR Heraeus centrifuge with LH-4000 rotor (Kendro Laboratory Products), washed twice with 70 % ethanol, re-dissolved in water and dialyzed against water (Molecular weight cut-off (MWCO) 3500 Da) at 4°C for 72h while the water was replaced several times. The remaining polymeric material was freeze dried and designated WAo (Water extract of *A.ovinus*). The residue after water extraction was treated twice with 1M NaOH added 0.135M $NaBH_4$ (1000 mL) at 100°C under reflux for 4h. The combined alkali extracts were precipitated with three volumes of ethanol and treated as described above. The isolated polymeric material was designated AAo (Alkali extract of *A. ovinus*). AAo was further separated into a water soluble fraction (AAoSw) and a remaining water insoluble fraction (AAoIw): AAo (1g/100mL water) was shaken on a water bath at 70°C for 40 min then sonicated (40 sec + 20 sec x 3 min, 90% amplitude) with a Sonics Vibra-cell ™ CV18 sonicator. The procedure was repeated once and left at 4°C over night and then centrifuged at 3500 rpm for 10 min. The pellet was washed twice with 70 % ethanol, dialyzed and finally lyophilized (AAoSP) while the supernatant was re-precipitated with 3 volumes of ethanol, dialyzed and freeze dried (AAoSSP).

3.2 SEC-HPLC

Size exclusion chromatography on HPLC was performed on a TSK-Gel® G5000PW_{XL} column (7.8 x 300 mm) with a PW_{XL} Guard column (6.0 x 40 mm) (Tosoh Bioscience LLC) coupled to a LaChrom Elite L-2200 autosampler and L-2130 HPLC pump. Elution profiles were recorded with a L-2490 RI detector, and the equipment was controlled by EZ LaChrom Elite software (Hitachi High Technologies America, Inc). Samples (1 mg/mL) were dissolved in 0.05M Na_2SO_4, filtered (0.45 µm) and aliquots of 95 µL were

injected onto the column and run at 0.5 mL/min with 0.05M Na_2SO_4 as the eluent. Molecule weights were determined using pullulan standards (Mp 853, 380, 186, 100, 48, 23.7, 12.2 and 5.8kDa; Polymer Laboratories LTD, Church Stretton, UK) measuring their peak retention times found under conditions as described and plotted vs lgMp preparing a standard curve (R^2=0.9969) used for Mp determination.

3.3 SEC-MALLS

The weight-average molecular weight of the water soluble fraction WAoF1 was determined by size exclusion chromatography with multi-angle laser light scattering (SEC-MALLS) as described previously [18]. This analysis was performed at Nofima, Norwegian Institute of Food, Fisheries and Aquaculture Research, Aas, Norway.

3.4 Preparative SEC

Preparative size exclusion chromatography (SEC) was performed on a Sephacryl S-500 column (26 x 940 mm) (GE-Healthcare Bio-sciences, Uppsala, Sweden) coupled to a Valve IV-7 (Pharmacia Biotech, Uppsala Sweden) and a P-50 pump (Pharmacia Biotech). The sample (WAo) was dissolved (1 mg/mL) in 0.05M NaCl, filtered (0.45 µm), injected onto the column and eluted with 0.05M NaCl at 1 mL/min. Fractions were collected with a SuperFrac fraction collector (Pharmacia Biotech) and pooled according to the elution profile recorded by a RID-6A detector (Shimadzu, Kyoto, Japan) monitored by Chromelion software version 7.0 (Dionex Corporation, Sunnyvale, California, US). The fractionation was repeated several times. Pooled fractions were dialyzed against water and lyophilized.

3.5 Monosaccharide composition

Monosaccharide composition was determined by methanolysis as described by Nyman et al.[18]

3.6 Linkage analysis

Analysis of glykosidic linkages was performed by methylation and GC-MS based on previously described methods [18, 46, 47].

3.7 Alpha-amylase treatment

Polysaccharide samples were dissolved in distilled water (2 mg/mL) and added alpha-amylase from barley malt (EC 3.2.1.1) (Sigma-Aldrich, Darmstadt, Germany), 0.5U/mg polysaccharide sample and 2 drops of toluene/50 mL solution as an antibacterial agent. Samples were incubated at 37°C for 2 h, then boiled on a hot water bath to terminate the reaction and added 3 volumes of ethanol for precipitation and left over night at 4°C then centrifuged at 3000 rpm (Multifuge® 4KR Heraeus centrifuge with LH-4000 rotor) for 10 min. The precipitate was washed 3 times with 70 % ethanol and centrifuged each time. The precipitate was finally dissolved in distilled water and freeze dried.

3.8 ConA Sepharose 4B Affinity chromatography

ConA Sepharose 4B (GE Healthcare) (5 mL) was washed with the Starting buffer (20 mM Tris-HCl, 0.5M NaCl, 1 mM $MnCl_2$, 1 mM $CaCl_2$, pH 7.4) according to the producers instructions, and 15 mg sample dissolved in 2 mL starting buffer was then added to the column. The non-binding fraction of the sample (ConA-) was washed from the column with 10 volumes of starting buffer while the ConA binding fraction (ConA+) was removed from the column with 5 volumes of Eluting buffer (0.2 M methyl-α-D-Man*p*, 20 mM Tris-HCl, 0.5 M NaCl, pH 7.4). The column material was regenerated and stored according to the producers instructions.

3.9 NMR

Polysaccharide samples (10 mg) were dissolved in 600 µL D_2O 99.9 % (Chiron, Trondheim, Norway) and added 5 µL 3-(trimethylsilyl)propionic 2,2,3,3,-d4 acid (Sigma Aldrich) as an internal reference. All homo- and heteronuclear NMR experiments were carried out on either a Bruker Avance IIIHD 800 MHz or Avance 600 MHz spectrometer (Bruker BioSpin AG, Fallanden, Switzerland) equipped with 5-mm cryogenic CP-TCI z-gradient probes at 339.6K.

For chemical shift assignment, the following spectra were recorded: 1D ^{1}H, 1D ^{1}H using the excitation sculpting scheme for water suppression, 1D ^{13}C, 2D double quantum filter correlated spectroscopy (DQF-COSY), 2D total correlation spectroscopy (TOCSY) with 70 ms mixing time and using the excitation sculpting scheme for water suppression, 2D nuclear Overhauser effect spectroscopy (NOESY) with 50 ms mixing time, 2D ^{13}C heteronuclear single quantum coherence (HSQC) with multiplicity editing and 2D^{13}C heteronuclear multiband correlation (HMBC) with BIRD filter to suppress first order correlation (with a 1J bond suppression filter optimized for 145 Hz).

The NMR-experiments used in the current investigations were generally not those supplied by Bruker. In house modified parameter files containing pulse programs adapted for solvent suppressions were employed. Description of the individual experiments can be found at [48, 49].

In house modified experiments with solvent suppression were applied, using the following pulse programs: zgpr, zgesgp, awcosygpprqf, mlevphpr, dipsi2phpr, awhsqcedetgpsisp2.3-135pr, awhmbcgplpndqfpr. The three pulse programs awcosygpprqf, awhsqcedetgpsisp2.3-135pr and awhmbcgplpndqfpr include solvent presaturation not supplied by Bruker[48, 50]. Copies of three modified pp's are available from the authors on request.

Band selective 2D experiments were used to improve resolution on the ^{13}C axis. The general description of these experiments is available in [49, 51]. The pulse programs: shsqcetgpsisp2.3-135 and shmbcq3.800 were employed.

The anomeric ^{13}C-^{1}H-coupling constant $^{1}J_{(C1,H1)}$ was determined by band selective HSQC without proton decoupling using the homemade parameter file; awshsqc135 (pulse program awshsqcetgpsisp2.3-135.) [49, 51].

1D-SELNOESY and SELROESY spectra were acquired using standard Bruker pulse programmes modified by the inclusion of CW presaturation of the HOD signal on F2 during d1 = 2.5 sec. Gradient assisted 2D-NOESY and CW spin locked ROESY spectra were acquired with presaturation of the HOD signal during d1 = 2 sec. 1D-SELNOESY and 2D-NOESY expts were performed with a mixing time (d8) of 0.07 sec. 1D-SELROESY and 2D-ROESY expts were performed with a CW spin locked time (P15) of 250000 usec.

The spectra were recorded using TopSpin 3.5 patch level 7 software (Bruker BioSpin) and processed and analyzed with TopSpin 3.2 software (Bruker BioSpin).

4. Acknowledgements

The authors thank Dr. Simon Balance, Nofima Food Research Institute for the SEC-MALLS analysis and Hoai Thi Nguyen Aas, School of Pharmacy for technical assistance. This work was partly supported by the Research Council of Norway through the Norwegian NMR Platform, NNP (226244/F50).

5. References

[1] F. Bach, C.V. Helm, M.B. Bellettini, G.M. Maciel, and C.W.I. Haminiuk, Edible mushrooms: a potential source of essential amino acids, glucans and minerals. Int J Food Sci Tech, 52 (2017) 2382-2392.

[2] P.C.K. Cheung, Nutritional Value and Health Benefits of Mushrooms, in Mushrooms as Functional Foods, P.C.K. Cheung, Editor. John Wiley & Sons Inc.: New Jersey, 2008, p. 71-109.

[3] H.A. El Enshasy and R. Hatti-Kaul, Mushroom immunomodulators: unique molecules with unlimited applications. Trends Biotechnol, 31 (2013) 668-677.

[4] S.E. Hardison and G.D. Brown, C-type lectin receptors orchestrate antifungal immunity. Nature Immunology, 13 (2012) 817-822.

[5] J.P. Latge, Tasting the fungal cell wall. Cellular Microbiology, 12 (2010) 863-872.

[6] A. Synytsya and M. Novak, Structural diversity of fungal glucans. Carbohydrate Polymers, 92 (2013) 792-809.

[7] F.M. Zhu, B. Du, Z.X. Bian, and B.J. Xu, Beta-glucans from edible and medicinal mushrooms: Characteristics, physicochemical and biological activities. J Food Compos Anal, 41 (2015) 165-173.

[8] X. Meng, H.B. Liang, and L.X. Luo, Antitumor polysaccharides from mushrooms: a review on the structural characteristics, antitumor mechanisms and immunomodulating activities. Carbohydrate Research, 424 (2016) 30-41.

[9] N. Dalonso, G.H. Goldman, and R.M. Gern, beta-(1-->3),(1-->6)-Glucans: medicinal activities, characterization, biosynthesis and new horizons. Appl Microbiol Biotechnol, 99 (2015) 7893-906.

[10] C.J. Qi, Y.H. Cai, L. Gunn, C.L. Ding, B. Li, G. Kloecker, K.Q. Qian, J. Vasilakos, S. Saijo, Y. Iwakura, et al., Differential pathways regulating innate and adaptive antitumor immune responses by particulate and soluble yeast-derived beta-glucans. Blood, 117 (2011) 6825-6836.

[11] M. Liu, F. Luo, C. Ding, S. Albeituni, X. Hu, Y. Ma, Y. Cai, L. McNally, M.A. Sanders, D. Jain, et al., Dectin-1 Activation by a Natural Product beta-Glucan Converts Immunosuppressive Macrophages into an M1-like Phenotype. J Immunol, 195 (2015) 5055-65.

[12] S.C. Cheng, J. Quintin, R.A. Cramer, K.M. Shepardson, S. Saeed, V. Kumar, E.J. Giamarellos-Bourboulis, J.H. Martens, N.A. Rao, A. Aghajanirefah, et al., mTOR- and HIF-1alpha-mediated aerobic glycolysis as metabolic basis for trained immunity. Science, 345 (2014) 1250684.

[13] H. Rathore, S. Presad, and S. Sharma, Mushroom nutraceuticals for improved nutrition and better human health: A review. PharmaNutrition 5(2017) 35-46.

[14] Y. Cao, Y. Sun, S.W. Zou, M.X. Li, and X.J. Xu, Orally Administered Baker's Yeast beta-Glucan Promotes Glucose and Lipid Homeostasis in the Livers of Obesity and Diabetes Model Mice. Journal of Agricultural and Food Chemistry, 65 (2017) 9665-9674.

[15] I. Roncero-Ramos and C. Delgado-Andrade, The beneficial role of edible mushrooms in human health. Curr Opin Food Sci, 14 (2017) 122-128.

[16] Y.Y. Zhang, S. Li, X.H. Wang, L.N. Zhang, and P.C.K. Cheung, Advances in lentinan: Isolation, structure, chain conformation and bioactivities. Food Hydrocolloids, 25 (2011) 196-206.

[17] N. Ohno, Yeast and Fungal Polysaccaharides, Analyis of Glycans polysaccharide functional properties. 1 ed. Comprehensive Glycoscience, Four-Volume Set, Chemistry to Systems Biology, ed. J. Kamerling. Vol. 2. Elsevier, Amsterdam 2007.

[18] A.A.T. Nyman, F.L. Aachmann, F. Rise, S. Ballance, and A.B.C. Samuelsen, Structural characterization of a branched (1→6)-α-mannan and β-glucans isolated from the fruiting bodies of *Cantharellus cibarius*. Carbohydrate Polymers, 146 (2016) 197-207.

[19] Y. Roman, M. Iacomini, G.L. Sassaki, and T.R. Cipriani, Optimization of chemical sulfation, structural characterization and anticoagulant activity of *Agaricus bisporus* fucogalactan. Carbohydrate Polymers, 146 (2016) 345-352.

[20] A.C. Ruthes, E.R. Carbonero, M.M. Cordova, C.H. Baggio, G.L. Sassaki, P.A.J. Gorin, A.R.S. Santos, and M. Iacomini, Fucomannogalactan and glucan from mushroom *Amanita muscaria*: Structure and inflammatory pain inhibition. Carbohydrate Polymers, 98 (2013) 761-769.

[21] Y. Meng, J. Yan, G. Yang, H. Cheng, and Y. Zhou, Structural characterization and macrophage activation of a hetero-galactan isolated from *Flammulina velutipes*. Carbohydrate Polymers, 183 (2018) 207-218.

[22] K. Axelsson and H. Bjorndal, Polysaccharides Elaborated by Polyporus Ovinus (Schaeff) .I. Structure of a Fucogalactan from Water Extracts of Fruit Bodies. Acta Chem Scand, 23 (1969) 1815-&.

[23] P.K. Agrawal, Nmr-Spectroscopy in the Structural Elucidation of Oligosaccharides and Glycosides. Phytochemistry, 31 (1992) 3307-3330.

[24] A.Q. Zhang, J.S. Zhang, Q.U. Tang, W. Jia, Y. Yang, Y.F. Liu, J.M. Fan, and Y.J. Pan, Structural elucidation of a novel fucogalactan that contains 3-O-methyl rhamnose isolated from the fruiting bodies of the fungus, *Hericium erinaceus*. Carbohydrate Research, 341 (2006) 645-649.

[25] J.M. Fan, J.S. Zhang, Q.J. Tang, Y.F. Liu, A.Q. Zhang, and Y.J. Pan, Structural elucidation of a neutral fucogalactan from the mycelium of *Coprinus comatus*. Carbohyd Res, 341 (2006) 1130-1134.

[26] K. Bock, C. Pedersen, and H. Pedersen, Carbon-13 nuclear magnetic resonance data for oligosaccharides, in Advances in carbohydrate chemistry and biochemistry. Academic Press, 1983, p. 193-224.

[27] A.C. Ruthes, Y.D. Rattmann, E.R. Carbonero, P.A.J. Gorin, and M. Iacomini, Structural characterization and protective effect against murine sepsis of fucogalactans from *Agaricus bisporus* and *Lactarius rufus*. Carbohydrate Polymers, 87 (2012) 1620-1627.

[28] A.C. Ruthes, Y.D. Rattmann, S.M. Malquevicz-Paiva, E.R. Carbonero, M.M. Cordova, C.H. Baggio, A.R.S. Santos, P.A.J. Gorin, and M. Iacomini, *Agaricus bisporus* fucogalactan: Structural characterization and pharmacological approaches. Carbohydrate Polymers, 92 (2013) 184-191.

[29] Y. Wang, X.K. Shen, W.F. Liao, J.P. Fang, X. Chen, Q. Dong, and K. Ding, A heteropolysaccharide, L-fuco-D-manno-1,6-alpha-D-galactan extracted from *Grifola frondosa* and antiangiogenic activity of its sulfated derivative. Carbohydrate Polymers, 101 (2014) 631-641.

[30] A.C. Ruthes, F.R. Smiderle, and M. Iacomini, Mushroom heteropolysaccharides: A review on their sources, structure and biological effects. Carbohydrate Polymers, 136 (2016) 358-375.

[31] E. Redel, C. Rohr, and C. Janiak, An inorganic starch-iodine model: the inorganic-organic hybrid compound {(C4H12N2)(2)[(CuI4)-I-I](I-2)}(n). Chemical communications, (2009) 2103-2105.

[32] G.H.L. Sciences, Con A Sepharose 4B, GE Healthcare Life Sciences. 2018, Available from: https://www.gelifesciences.com/shop/chromatography/resins/affinity-specific-groups/con-a-sepharose-4b-p-05883?current=17044001 (accessed 13 August 2018).

[33] M.J. Frampton, T.D.W. Claridge, G. Latini, S. Brovelli, F. Cacialli, and H.L. Anderson, Amylose-wrapped luminescent conjugated polymers. Chemical communications, (2008) 2797-2799.

[34] M. Lundborg and G. Widmalm, Structural Analysis of Glycans by NMR Chemical Shift Prediction. Analytical Chemistry, 83 (2011) 1514-1517.

[35] I. Palacios, A. Garcia-Lafuente, E. Guillamon, and A. Villares, Novel isolation of water-soluble polysaccharides from the fruiting bodies of *Pleurotus ostreatus* mushrooms. Carbohydrate Research, 358 (2012) 72-77.

[36] F.R. Smiderle, G.L. Sassaki, J. van Arkel, M. Iacomini, H.J. Wichers, and L.J.L.D. van Griensven, High Molecular Weight Glucan of the Culinary Medicinal Mushroom *Agaricus bisporus* is an alpha-Glucan that Forms Complexes with Low Molecular Weight Galactan. Molecules, 15 (2010) 5818-5830.

[37] Y. Masuda, Y. Nakayama, A. Tanaka, K. Naito, and M. Konishi, Antitumor activity of orally administered maitake alpha-glucan by stimulating antitumor immune response in murine tumor. PloS one, 12 (2017)

[38] J.M. Yan, Z. Han, Y.H. Qu, C. Yao, D.Y. Shen, G.H. Tai, H.R. Cheng, and Y.F. Zhou, Structure elucidation and immunomodulatory activity of a beta-glucan derived from the fruiting bodies of *Amillariella mellea*. Food Chemistry, 240 (2018) 534-543.

[39] D.K. Manna, A.K. Nandi, M. Pattanayak, P. Maity, S. Tripathy, A.K. Mandal, S. Roy, S.S. Tripathy, N. Gupta, and S.S. Islam, A water soluble beta-glucan of an edible mushroom *Termitomyces heimii*: Structural and biological investigation. Carbohydrate Polymers, 134 (2015) 375-384.

[40] P. Bystricky, D. Dobrota, P. Racay, and S. Bystricky, NMR characteristics of alpha-D-Man-(1 -> 2)-D-Man and alpha-D-Man-(1 -> 3)-D-Man mannobioses related to *Candida albicans* yeast mannan structures. Chem Pap, 71 (2017) 2485-2493.

[41] K.K. Maity, S. Patra, B. Dey, S.K. Bhunia, S. Mandal, D. Das, D.K. Majumdar, S. Maiti, T.K. Maiti, and S.S. Islam, A heteropolysaccharide from aqueous extract of an edible mushroom, *Pleurotus ostreatus* cultivar: structural and biological studies. Carbohydrate Research, 346 (2011) 366-372.

[42] Y. Zhang, H. Kong, Y. Fang, K. Nishinari, and G.O. Phillips, Schizophyllan: A review on its structure, properties, bioactivities and recent developments. Bioactive Carbohydrates and Dietary Fibre, 1 (2013) 53-71.

[43] S. Karacsonyi and L. Kuniak, Polysaccharides of *Pleurotus-Ostreatus* - Isolation and Structure of Pleuran, an Alkali-Insoluble Beta-D-Glucan. Carbohydrate Polymers, 24 (1994) 107-111.

[44] S.M. Bowman and S.J. Free, The structure and synthesis of the fungal cell wall. Bioessays, 28 (2006) 799-808.

[45] J. Ruiz-Herrera, Fungal cell wall: Structure, Synthesis and Assembly. CRC Press, Florida US 1991.

[46] I. Ciucanu and F. Kerek, A Simple and Rapid Method for the Permethylation of Carbohydrates. Carbohyd Res, 131 (1984) 209-217.

[47] F.A. Pettolino, C. Walsh, G.B. Fincher, and A. Bacic, Determining the polysaccharide composition of plant cell walls. Nat Protoc, 7 (2012) 1590-1607.

[48] E. Johnson. Faster, Higher Resolution Spectra. in *Bruker SMASH Workshop*. 2016. La Jolla, CA: Bruker Available from: www.mn.uio.no/kjemi/english/research/about/infrastructure/nmr/manuals/miscellaneous/faster__higher_resolution_spectra.pdf (accessed 13 August 2018).

[49] Deptartment of Chemistry, NMR Manuals, University of Oslo, 2018, Available from: www.mn.uio.no/kjemi/english/research/about/infrastructure/nmr/manuals/KJM%209250%20from%20spring%202018/?page=2&u-page=2 (accessed 13 August 2018).

[50] A.L. Wilkins, ^{1}H NMR Spectra on the AVIIIHD-800, KJM 9250 University of Oslo. 2018, Available from: https://figshare.com/articles/NMR_with_solvent_suppression/6982709 (accessed 13 August 2018).

[51] A.L. Wilkins, SHSQC and SHMBC Experiments on the AVIIIHD800, KJM 9250 University of Oslo. 2018, Available from: https://figshare.com/articles/SHSQC_and_SHMBC_ALW_pdf/6982511 (accessed 13 August 2018).

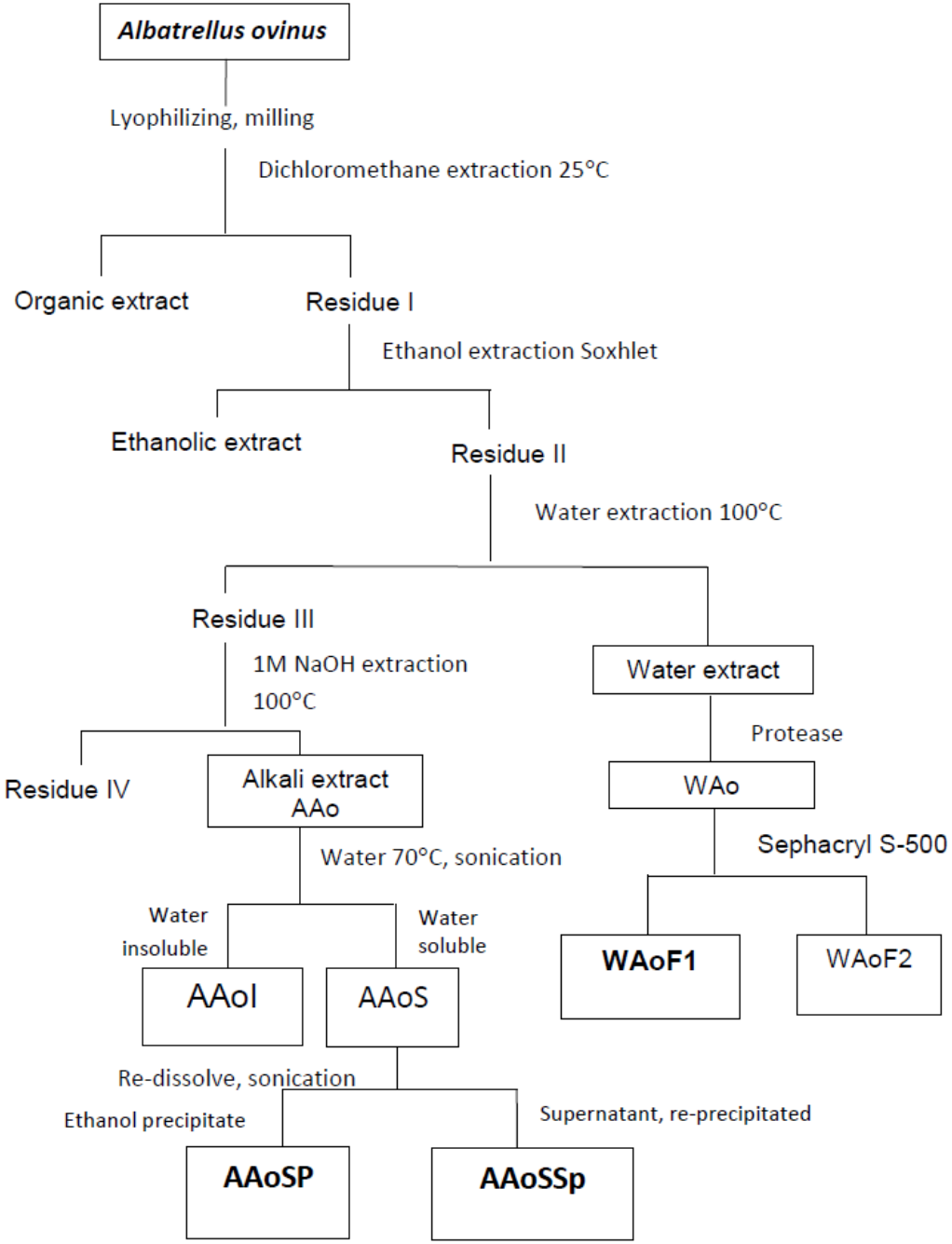

Fig.1 Flow diagram of the extraction of *Albatrellus ovinus* fruiting bodies. The detailed extraction procedure is found in chapter 3.1 Extraction

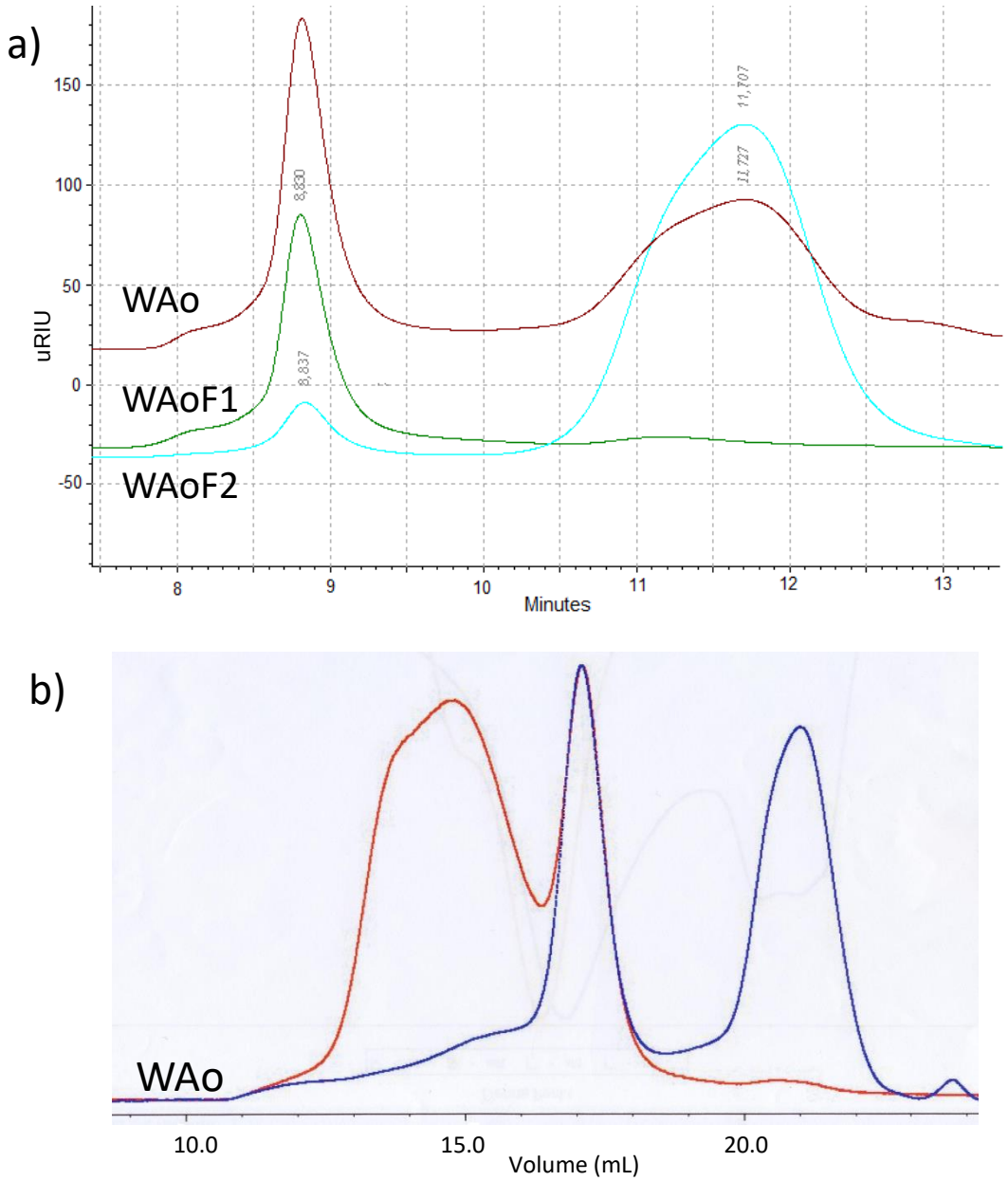

Fig. 2 SEC-HPLC of water extract Wao. a) RI profiles of WAo (upper trace), WAoF1 (middle trace) and WAoF2 (lower trace) recorded from a TSK-Gel® G5000PW$_{XL}$ column. b) SEC-MALLS profile of WAo; RI profile (blue trace) and light scattering signals (red trace) on serially connected TSK-Gel® G5000PW$_{XL}$ and G6000PW$_{XL}$ columns.

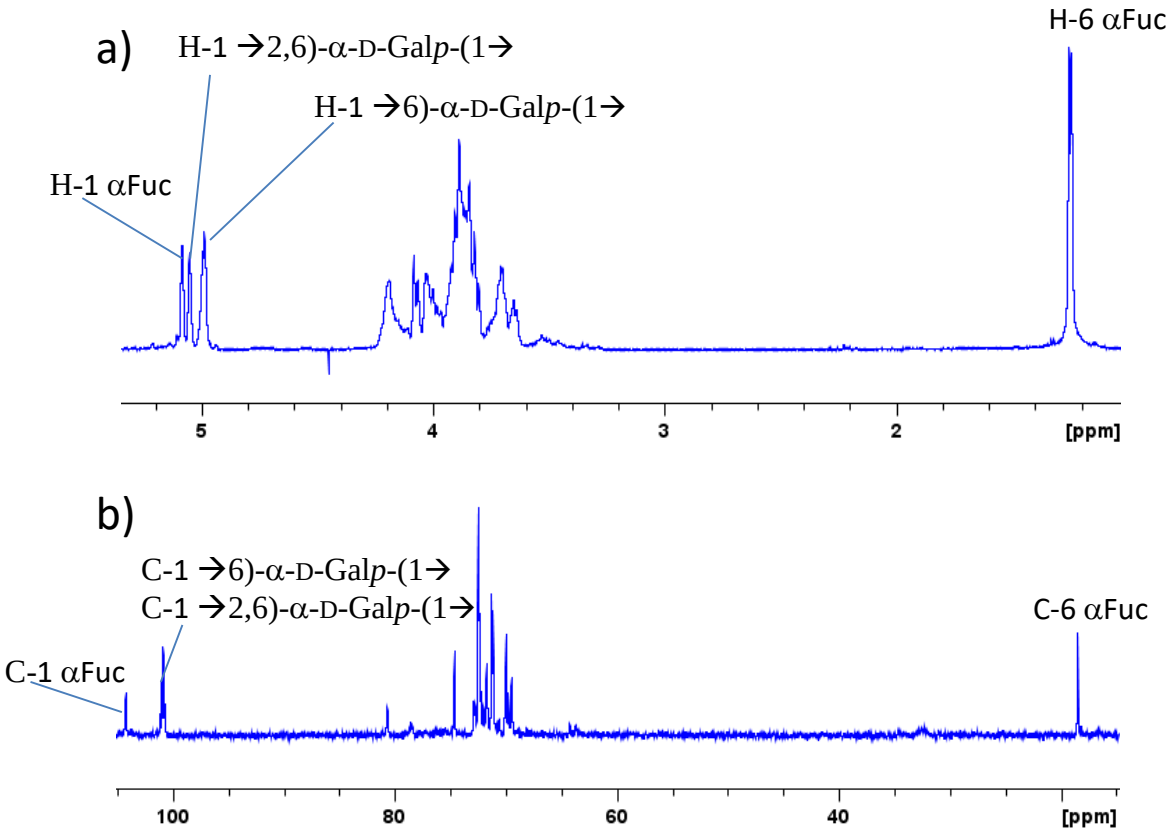

Fig. 3 ABCSamuelsen
Fig3 Albatrellus ovinus REV.jpg

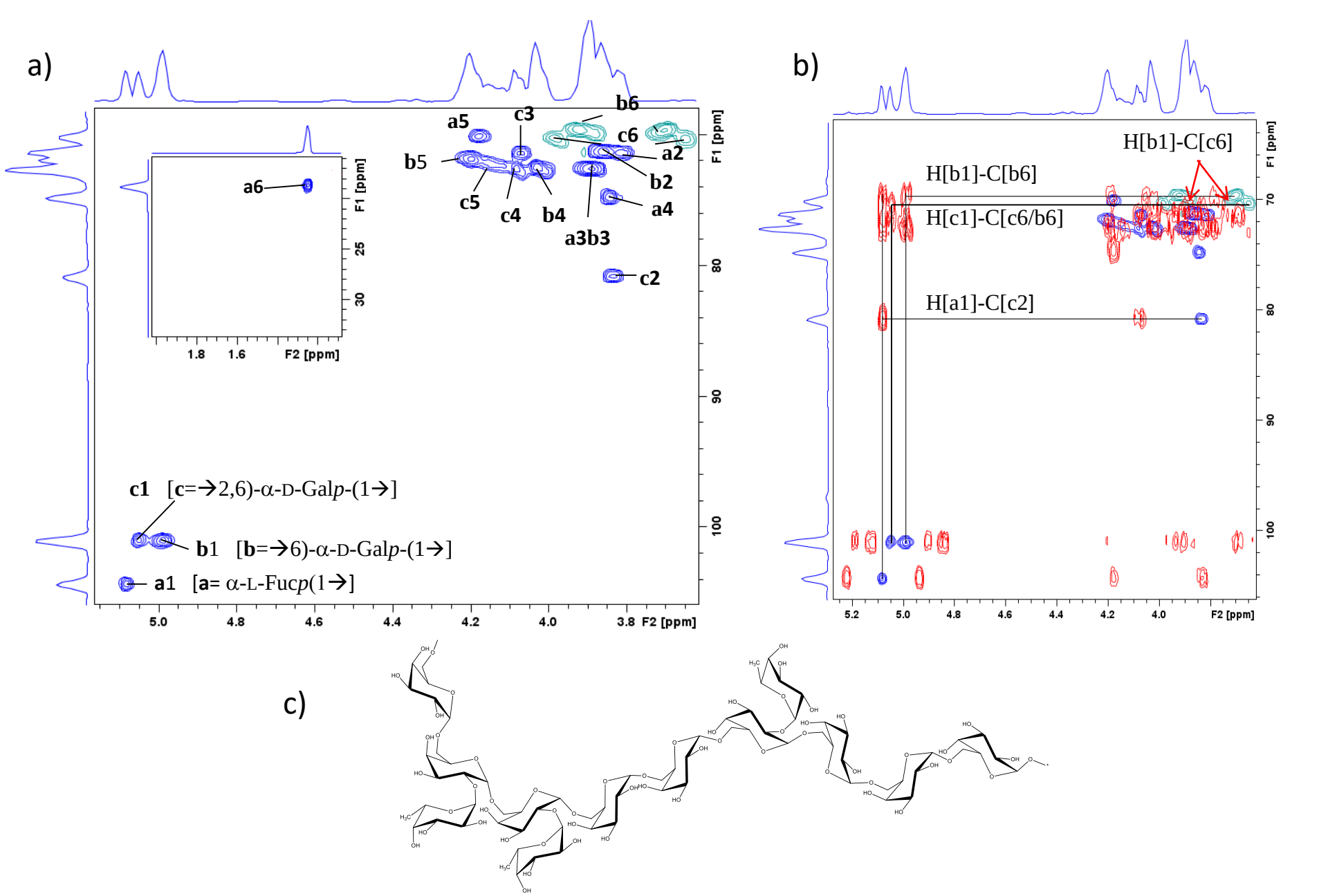

Fig. 4 ABCSamuelsen
Fig4 Albatrellus ovinus REV.jpg

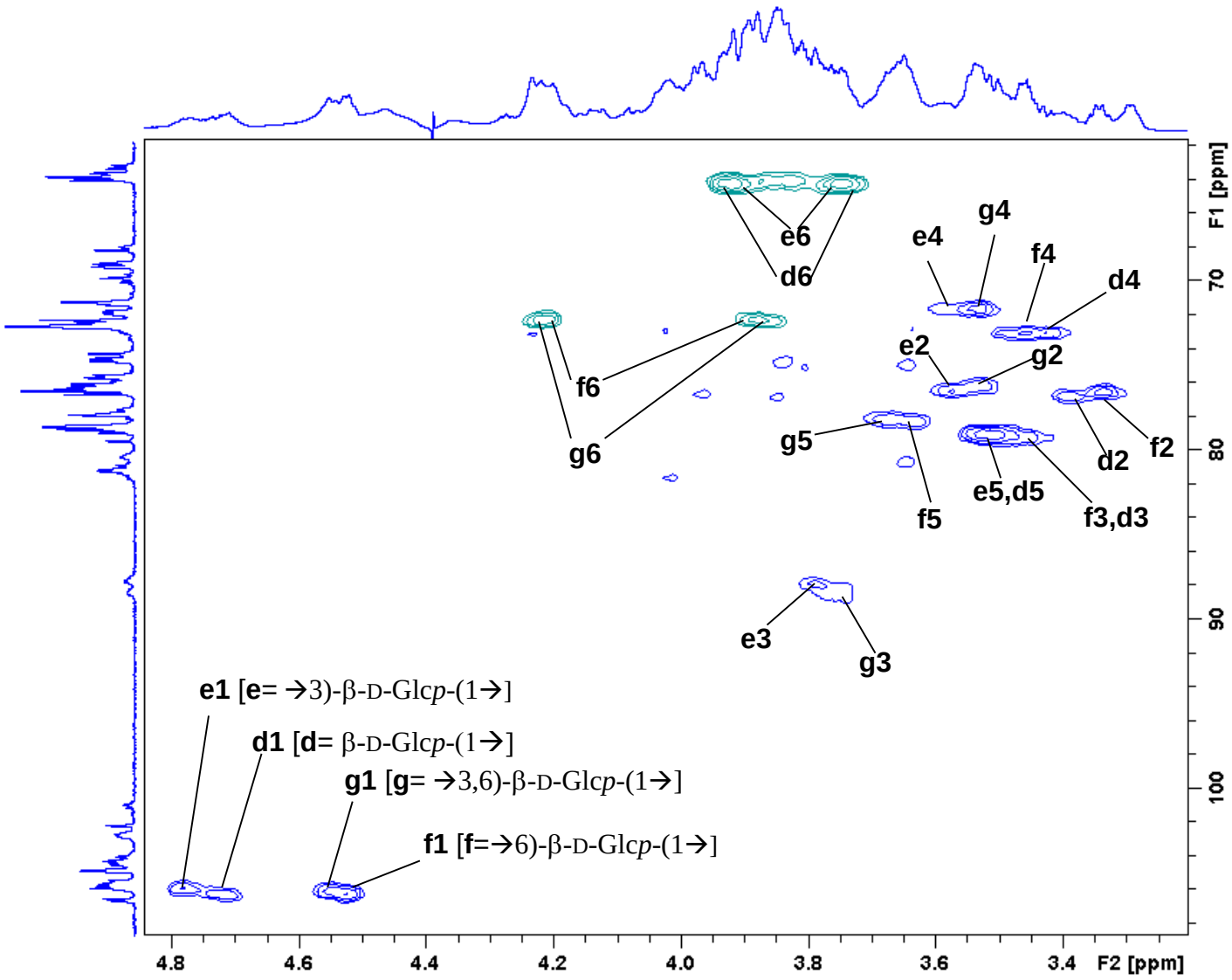

Fig 5a ABCSamuelsen
Fig5a Albatrellus ovinus REV.jpg

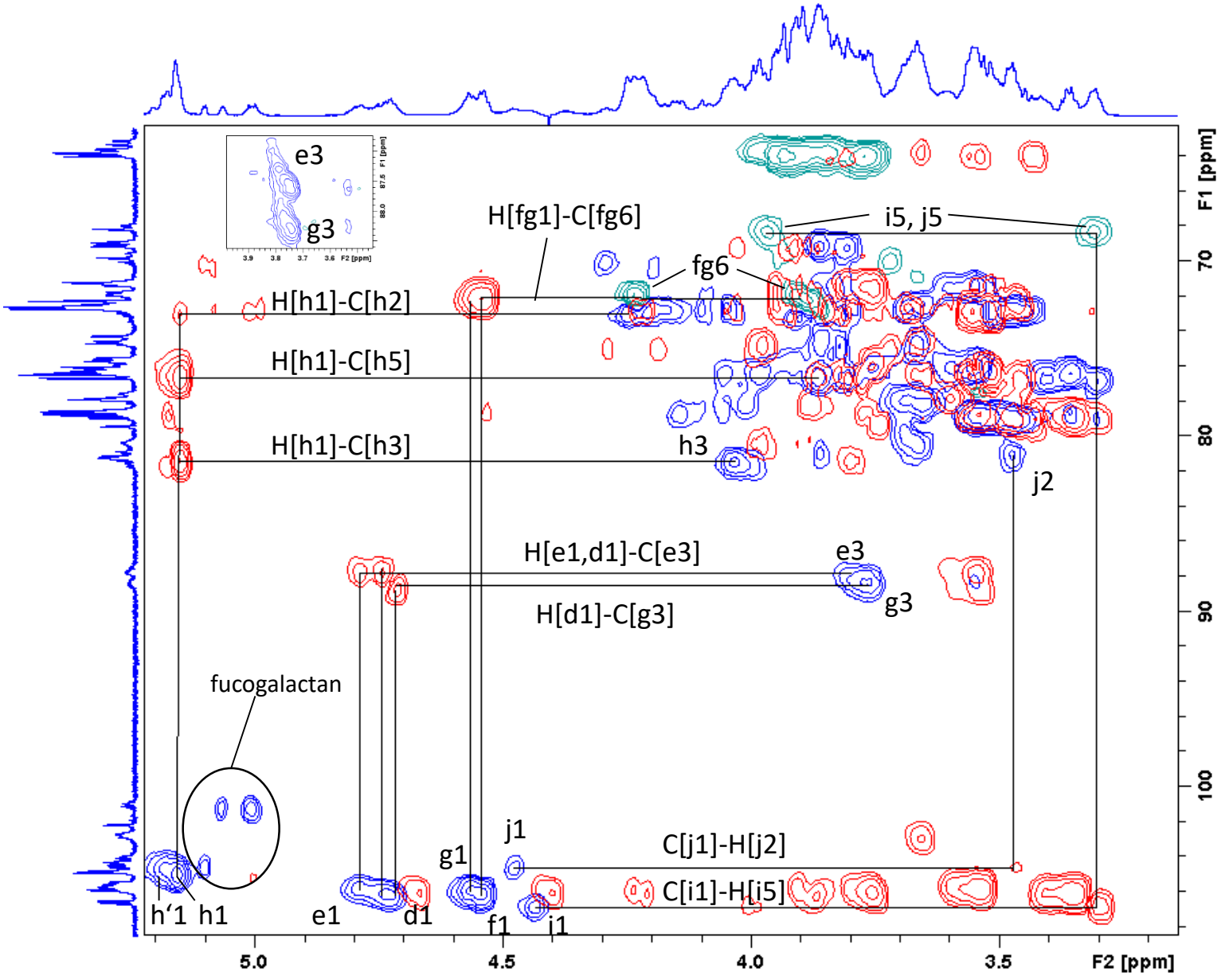

Fig. 5b ABCSamuelsen
Fig5b Albatrellus ovinus.jpg

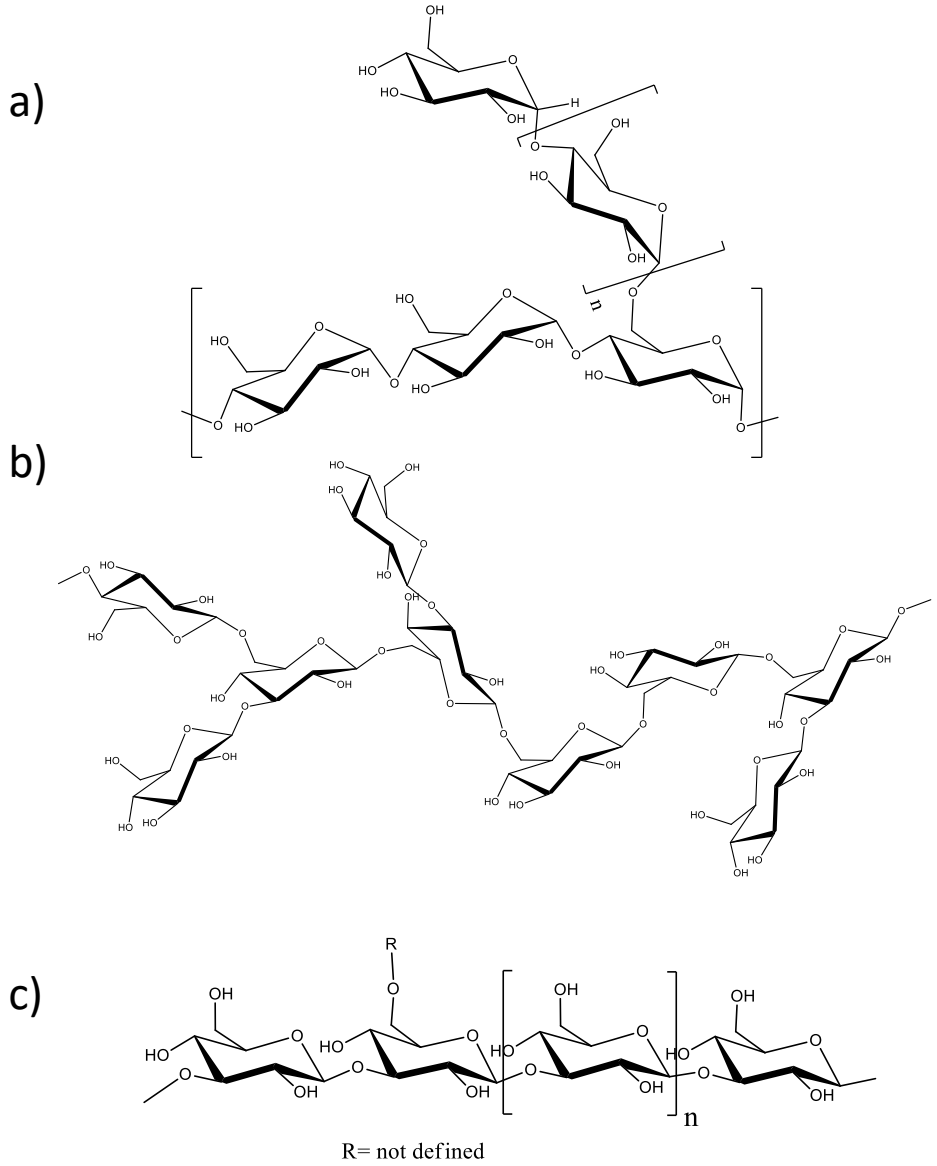

Fig. 6 ABCSamuelsen
Fig6 Albatrellus ovinus.jpg

Figure legends to CAR_2018_420

"The edible mushroom *Albatrellus ovinus* contains a α-L-fuco-α-D-galactan, α-D-glucan, a branched (1→6)-β-D-glucan and a (1→3)-β-D-glucan "

Fig. 1 Flow diagram of the extraction of *Albatrellus ovinus* fruiting bodies. The detailed extraction procedure is found in chapter 3.1 Extraction

Fig. 2 SEC-HPLC of water extract Wao. a) RI profiles of WAo (upper trace), WAoF1 (middle trace) and WAoF2 (lower trace) recorded from a TSK-Gel® G5000PW$_{XL}$ column. b) SEC-MALLS profile of WAo; RI profile (blue trace) and light scattering signals (red trace) on serially connected TSK-Gel® G5000PW$_{XL}$ and G6000PW$_{XL}$ columns.

Fig. 3 WAoF1 a) ^{1}H-NMR spectrum. b) ^{13}C-NMR spectrum

Fig. 4 a) Phase sensitive (CH blue, CH$_2$ green) HSQC NMR spectrum of the fucogalactan in WAoF1. Cross peaks are labelled as hexose monomers a = α-L-Fuc*p*(1→, b = →6)-α-D-Gal*p*-(1→ and c = →2,6)-α-D-Gal*p*-(1→, and numbers 1-6 are referring to H/C number on each monomer. E.g. a2 = cross peak of H/C number 2 on α-L-Fuc*p*(1→. **b)** HMBC cross peaks (red) overlay on HSQC of WAoF1. c) Proposed representative structure of the fucogalactan found.

Fig. 5a Phase sensitive HSQC (CH signals blue, CH$_2$ signals green) of β-glucans in AAoSP. Cross peaks are labelled as hexose monomers: d = β-D-Glc*p*-(1→, e = →3)-β-D-Glc*p*-(1→, f = →6)-β-D-Glc*p*-(1→, and g = →3,6)-β-D-Glc*p*-(1→ numbered 1-6 referring to monosaccharide H/C numbering. E.g. e3 = cross peak from H/C-3 on →3)-β-D-Glc*p*-(1→.

Fig. 5b Phase sensitive HSQC (CH$_2$-signals green, CH-signals blue) with HMBC (red) overlay of β-D-xylan, α-D-mannan and β-D-glucans in AAoSSp. d = β-D-Glc*p*-(1→), e = →3)-β-D-Glc*p*-(1→, f = →6)-β-D-Glc*p*-(1→, g = →3,6)-β-D-Glc*p*-(1→, h = →3)-α-D-Man*p*-(1→, h'= β-D-Xyl*p* (1→3)-α-D-Man*p*-(1→, i = β-D-Xyl*p*-(1→, j = →2)-β-D-Xyl*p*-(1→. Numbers refer to monosaccharide H/C-numbering

Fig. 6 Proposed representative structures of D-glucans in *Albatrellus ovinus*. a) (1→4)-α-D-glucan b) (1→6)-β-D-glucan c) (1→3)-β-D-glucan with undefined branches

Table 1a. *Semi-quantitative linkage distribution (%) and molecular weight of water extracted polysaccharide fractions from Albatrellus ovinus (WAo). WAoConA+ = WAo components with affinity to ConA, WAoConA- = WAo components without affinity to ConA*

Monomer	WAo	WAoConA+	WAoConA-	WAoF1	WAoF2
L-Fuc*p*-(1→	14	4	14	15	6
D-Gal*p*-(1→	2	7	4	2	0
→6)-D-Gal*p*-(1→	27	8	33	40	15
→2,6)-D-Gal*p*-(1→	13	0	13	18	7
→3)- D-Man*p*-(1→	3	2	5	5	3
D-Xyl*p*-(1→	0	0	2	0	0
→2)-D-Xyl*p*-(1→	0	0	0	0	0
D-Glc*p*-(1→	9	2	3	3	18
→3)-D-Glc*p*-(1→	6	3	16	7	6
→6)-D-Glc*p*-(1→	2	6	1	1	5
→3,4)-D-Glc*p*-(1→	1	4	1	0	0
→3,6)-D-Glc*p*-(1→	2	5	5	3	3
→4)-D-Glc*p*-(1→	17	46	3	3	25
→4,6)-D-Glc *p*-(1→	4	12	0	3	12
Mw(kDa) SEC-HPLC				251	12,4

Table 1b. *Semi quantitative linkage distribution (%) and molecular weight of alkali extracted polysaccharide fractions from Albatrellus ovinus (AAo). AAoI=water insoluble fraction, AAoS= water soluble fraction, AAoSP= Precipitate from re-dissolved soluble alkali extract AAoSSp= supernatant from re-dissolved soluble alkali extract.*

Monomer	AAoI	AAoS	AAoSP	AAoSSp
L-Fuc*p*-(1→	1	2	1	4
D-Gal*p*-(1→	trace	trace	0	trace
→6)-D-Gal*p*-(1→	1	2	0	2
→2,6)-D-Gal*p*-(1→	trace	1	0	1
→3)-D-Man*p*-(1→	12	12	4	25
D-Xyl*p*-(1→	4	3	1	4
→2)-D-Xyl*p*-(1→	2	trace	1	4
D-Glc*p*-(1→	8	12	28	3
→3)-D-Glc*p*-(1→	34	35	47	14
→6)-D-Glc*p*-(1→	3	6	2	6
→3,4)-D-Glc*p*-(1→	4	3	1	0
→3,6)-D-Glc*p*-(1→	15	7	10	3
→4)-D-Glc*p*-(1→	8	15	5	27
→4,6)-D-Glc*p*-(1→	0	2	0	0
Mw(kDa) SEC-HPLC	287	325	100	

Table 2. *NMR assignments of the fucogalactan in WAoF1.*

	Monomer	Position	$\delta^{1}H$	$\delta^{13}C$	NOESY	TOCSY	HMBC
a	α-L-Fuc-(1→	1	5.08	104.3	a2, c2	a2, a3, a4	c2, a3, a5
		2	3.82	71.3	a1, c3		
		3	3.89	72.6	a5		a1
		4	3.84	74.7	a5, a6		
		5	4.18	70.1	a3		a1
		6	1.25	18.6	a4, a5		
b	→6)-α-D-Gal-(1→*	1	4.99	101.0	b2, b6, c6	b2, b3, b4	b3, b5, b6
		2	3.86	71.2	b1		
		3	3.89	72.6	b4, b5		
		4	4.03	72.5	b3, b5		
		5	4.20	71.8	b3, b4, b6		b6
		6*	3.92/3.70	69.6	b1, b4, c1		b5
c	→2,6)-α-D-Gal-(1→**	1	5.05	101.0	c2, c6, b6	c2, c3, c4	c6
		2	3.84	80.8	c1, a1		a1
		3	4.07	71.4			
		4	4.08	72.6			
		5	4.15	72.2			
		6**	3.98/3.65	70.3	c1, b1		

*b and c linked to b, **b and c linked to c

Table 3. *NMR assignments of the from Albatrellus ovinus α-glucan that binds ConcanavalinA (fraction WAoConA+)*

		WAoConA+		Amylose (Sigma)	
Monomer	**Position**	**δ^1H**	**δ^{13}C**	**δ^1H**	**δ^{13}C**
→4)-α-D-Glc-(1→	1	5.36	103.2	5.39	102.6
	2	3.61	74.9	3.65	74.5
	3	3.98	76.6	3.97	76.2
	4	3.66	81.2	3.66	80.2
	5	3.86	74.5	3.85	74.2
	6	3.83/3.88	64.0	3.82/3.88	63.5
→4,6)-α-D-Glc-(1→	1	5.36	103.2	5.39	102.6
	2	3.61	74.9	3.6	74.4
	3	4.02	76.6	4.02	76.4
	4	3.6	81.6	3.61	81.4
	5	4.04	73.2	4.04	73.4
	6	3.65/3.97	70.7	3.66/3.95	70.6
α-D-Glc-(1→	1	4.98	101.5	4.98	101.5
	2	3.61	74.9	3.65	74.5
	3	3.73	76.2	3.72	75.8
	4	3.43	72.8	3.43	72.4
	5	na*	na	na	na
	6	3.82/3.88	64.0	3.82/3.88	63.5

*not assigned

Table 4. *NMR assignments of β-glucans in Albatrellus ovinus.* Underlined assignments were confirmed by selective NOESY.

	Monomer	postition	δ^1H	δ^{13}C	NOESY	HMBC	ROESY
d	β-D-Glc-(1→	1	4.72	106.1	g3, e3, d5	d3, d5, e3, g3	e3, d5
		2	3.39	76.7			
		3	3.47	79.1			
		4	3.43	73.0			
		5	3.52	78.9			
		6	3.75/3.92	64.2			
e	→3)-β-D-Glc-(1→	1	4.79	105.8	e3, e5	e3, g3	e3,e5
		2	3.57	76.5			
		3	3.79	87.8	e5		
		4	3.59	71.6			
		5	3.52	78.9	e3		
		6	3.75/3.92	64.2			
f	→6)-β-D-Glc(1→	1	4.53	106.2	f3, f5, f6, g3	f3, f5, f6, g6	f2, f5,f6
		2	3.34	76.5			
		3	3.47	79.1			
		4	3.46	73			
		5	3.64	78.3			
		6	4.23/3.89	72.2			
g	→3,6)-β-D-Glc-(1→	1	4.56	106	g3, g5, e5	e3, f6,	g5,f6
		2	3.53	76.1			
		3	3.75	88.3			
		4	3.53	71.6			
		5	3.67	78.2			
		6	4.22/3.87	72.0	g1		
h	→3)-α-D-Man-(1→	1	5.16	104.9	h2, h3, h4, h5	h3,h5,h6,	h2,h3,h4,h5
		2	4.25	73.0	h1, h3		
		3	4.03	81.4	h2, h5		
		4	3.81	69.1			
		5	3.87	76.6	h3		
		6	3.78/3.9	64.0			
h'	α-D-Man-(1→	1	5.18	104.5	h'2, h3, h2, h5	h'3, h'5	h3, h’2
		2	4.18	72.5	h3		
		3	4.05	72.8			

		4	3.87	69.0			
		5	3.81	76.7			
		6	3.78/3.9	64.0			
i	β-D-Xyl-(→	1	4.43	106.7	j2, i3, i5, h'3, h'4	i5, h'3	j2,i5,h5
		2	3.3	76.8			
		3	3.47	78.9	i5, i1		
		4	3.65	72.4			
		5	3.97/3.31	68.2	i4, i2		
j	→2)-β-D-Xyl-(1→	1	4.47	104.6	j5	j2	j2,j5
		2	3.48	81.6	j5		
		3	3.69	78.0			
		4	3.69	72.6			
		5	3.97/3.31	68.2	j2		